Supplementary Information (SI) for Polymer Chemistry.
This journal is © The Royal Society of Chemistry 2024

Ethylene-Bridged Bisisoindigo-Based Conjugated Polymers: Influence of Intramolecular CH···N Hydrogen Bonds

Keli Shi,[a,b] Jing Lai,[b] Qianqian Zhao,[b] Weifeng Zhang,*[,a,c] Qian Che,[a,c] Jiadi Chen,[d] Zhihui Chen,[a] Liping Wang,[d] and Gui Yu*[,a,c]

* Corresponding Author

[a]Beijing National Laboratory for Molecular Sciences, CAS Research/Education Center for Excellence in Molecular Sciences, Institute of Chemistry, Chinese Academy of Sciences, Beijing 100190, People's Republic of China

E-mail: zhangwf@iccas.ac.cn, yugui@iccas.ac.cn

[b]College of Physics and Electronic Information Engineering, Zhejiang Normal University, Zhejiang 321004, People's Republic of China

[c]School of Chemical Sciences, University of Chinese Academy of Sciences, Beijing 100049, People's Republic of China

[d]School of Material Science and Engineering, University of Science and Technology Beijing, Beijing 100083, People's Republic of China

† Electronic supplementary information (ESI) available. See DOI:

Instruments and Characterization

The ^{1}H NMR spectra of polymer materials were collected on a Bruker Avance III 400 NMR spectrometer at 110 °C. The gel permeation chromatography (GPC) analyses

were performed on a Polymer Labs PL 220 system (Agilent, USA) at 150 °C using 1, 2, 4-trichlorobenzene (TCB) as the eluent and polystyrenes as the standard, respectively. The elemental analyses were conducted on a Carlo Erba 1106 Elemental Analyzer (Carlo-Erba, Italy). The thermogravimetric analyses (TGA) were conducted on a Perkin–Elmer series 7 thermal analysis system (Perkin Elmer, USA) under N_2 at a heating rate of 10 °C min^{-1}. The differential scanning calorimetry (DSC) analyses were performed on a Mettler Toledo Instrument DSC822 calorimeter (Mettler Toledo, Switzerland). The UV−vis−NIR absorption spectra of polymer materials (in dilute solution and as thin film) were recorded on a Hitachi U-3010 spectrophotometer (Hitachi, Japan). The cyclic voltammetry (CV) curves were collected on a CHI660c electrochemistry workstation (Chenhua, China) with a conventional three-electrode configuration in dry acetonitrile containing 0.1 M *n*-Bu_4NPF_6 using platinum stick electrode, Ag/AgCl electrode, and platinum wire as working, reference, and counter electrodes, respectively. The CV measurements were carried out at room temperature under argon atmosphere and the respective thin films of these polymers were coated on the working electrode from the polymer solution in dichlorobenzene. The ultraviolet photoelectron spectroscopy (UPS) measurements were carried out on an Axis-Nova CJ109 X-ray photoelectron spectrometer (Kratos, UK). The thin film surface morphologies were determined on a Digital Instruments Nanoscope V atomic force microscope (Digital Instruments, USA) operated in tapping mode. The 2D grazing-incidence wide-angle X-ray scattering (2D-GIWAXS) data were acquired at beamline BL14B1 of the Shanghai Synchrotron Radiation Facility (SSRF).

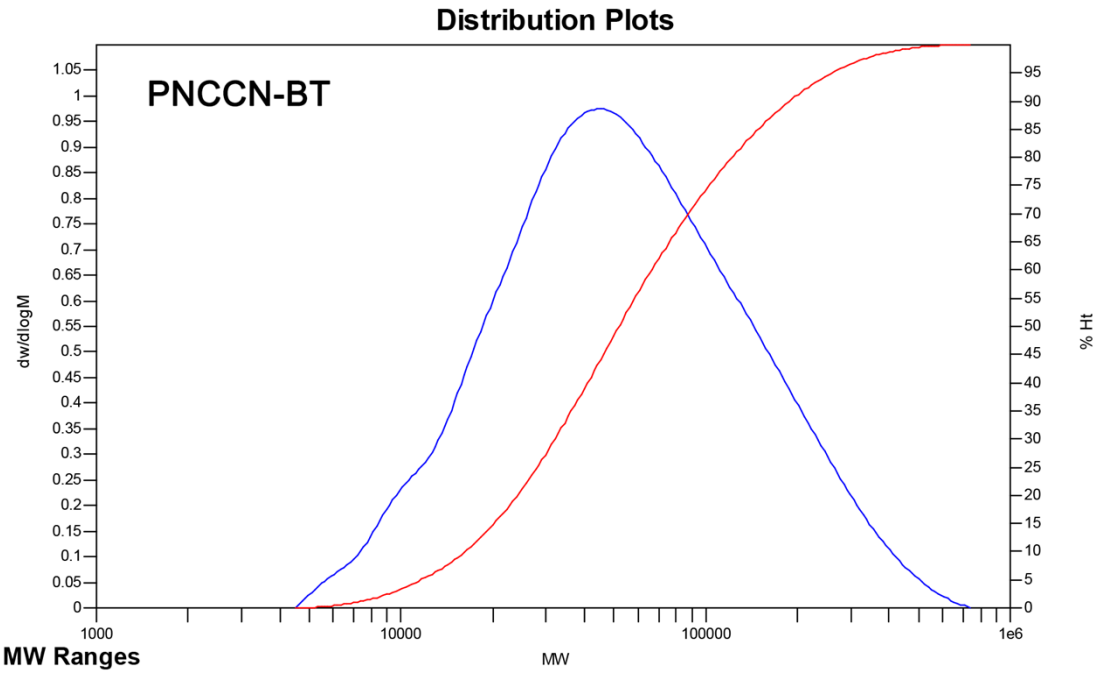

Figure S1. GPC plot of the bisisoindigo-based conjugated polymer **PNCCN-BT**.

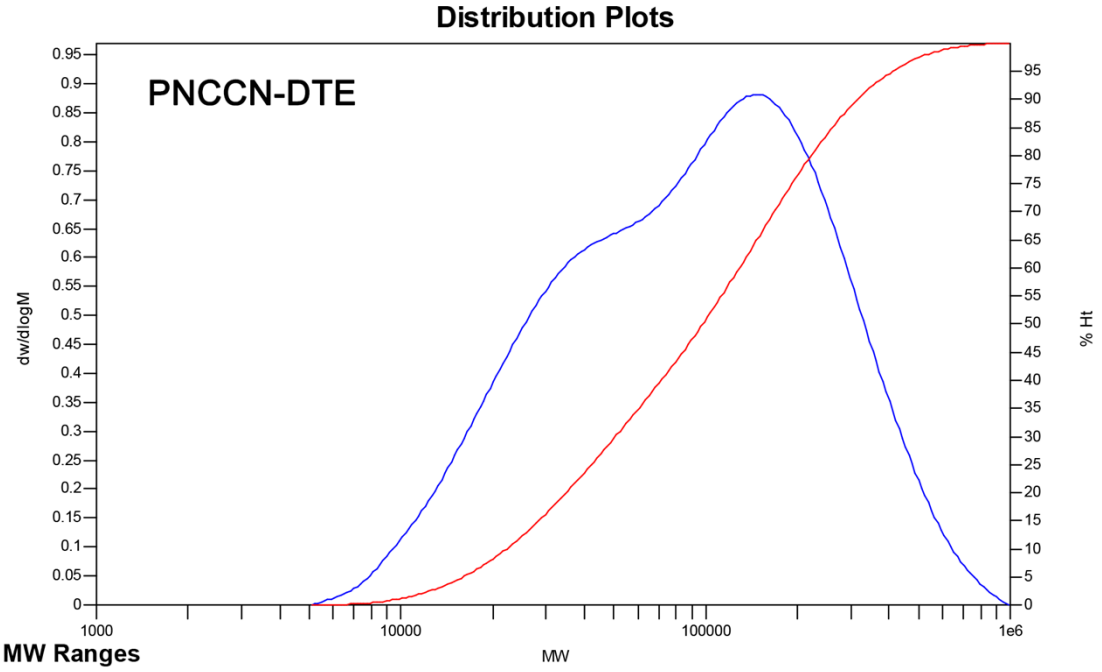

Figure S2. GPC plot of the bisisoindigo-based conjugated polymer **PNCCN-DTE**.

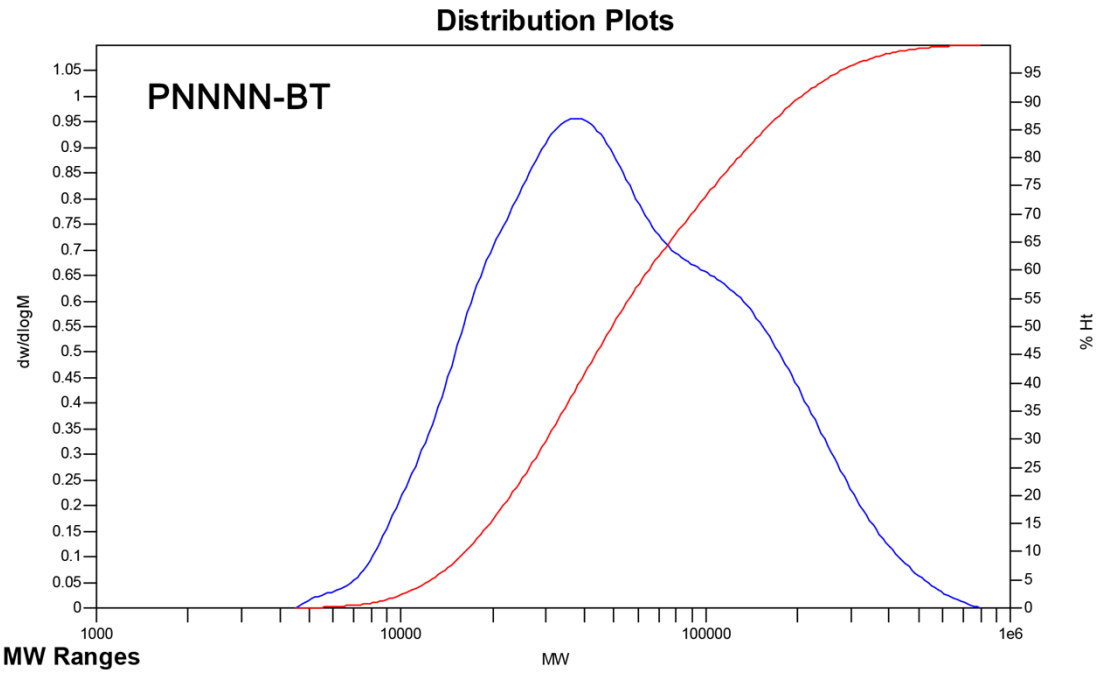

Figure S3. GPC plot of the bisisoindigo-based conjugated polymer **PNNNN-BT**.

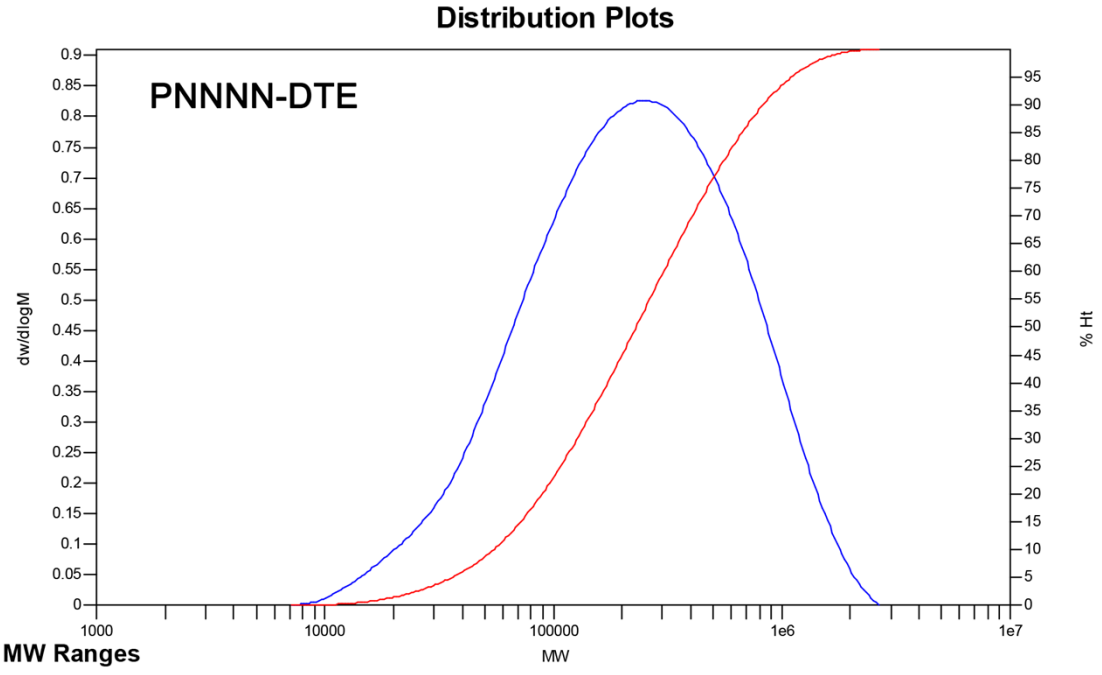

Figure S4. GPC plot of the bisisoindigo-based conjugated polymer **PNNNN-DTE**.

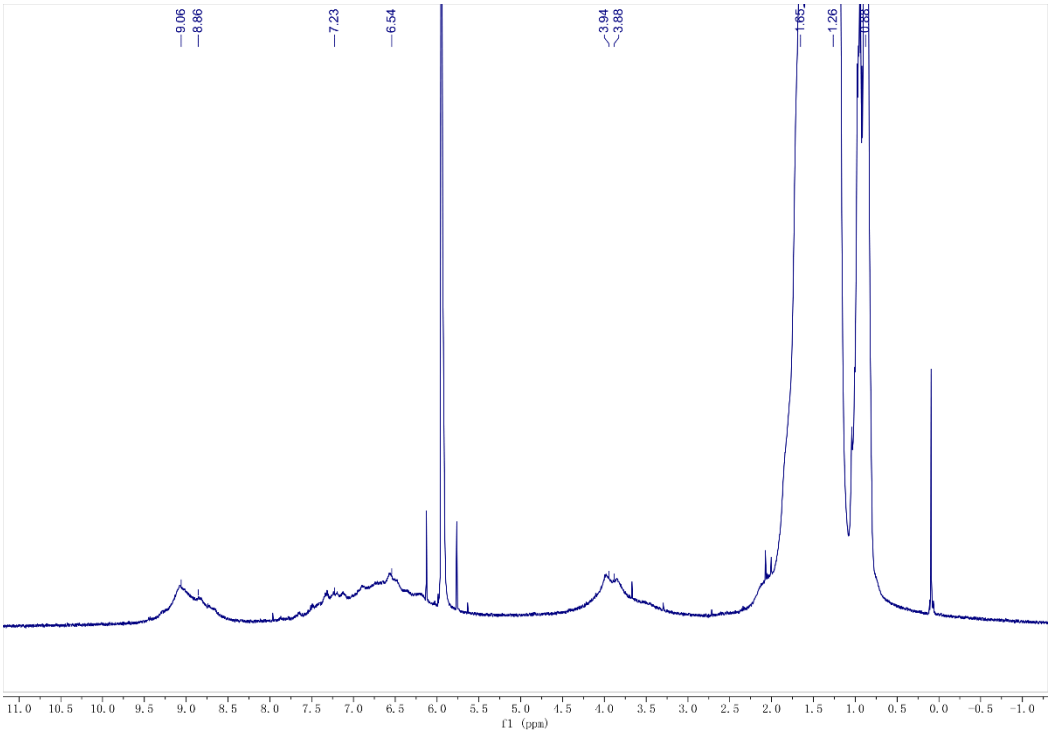

Figure S5. High temperature ^{1}H NMR spectrum of the bisisoindigo-based conjugated polymer **PNCCN-BT**.

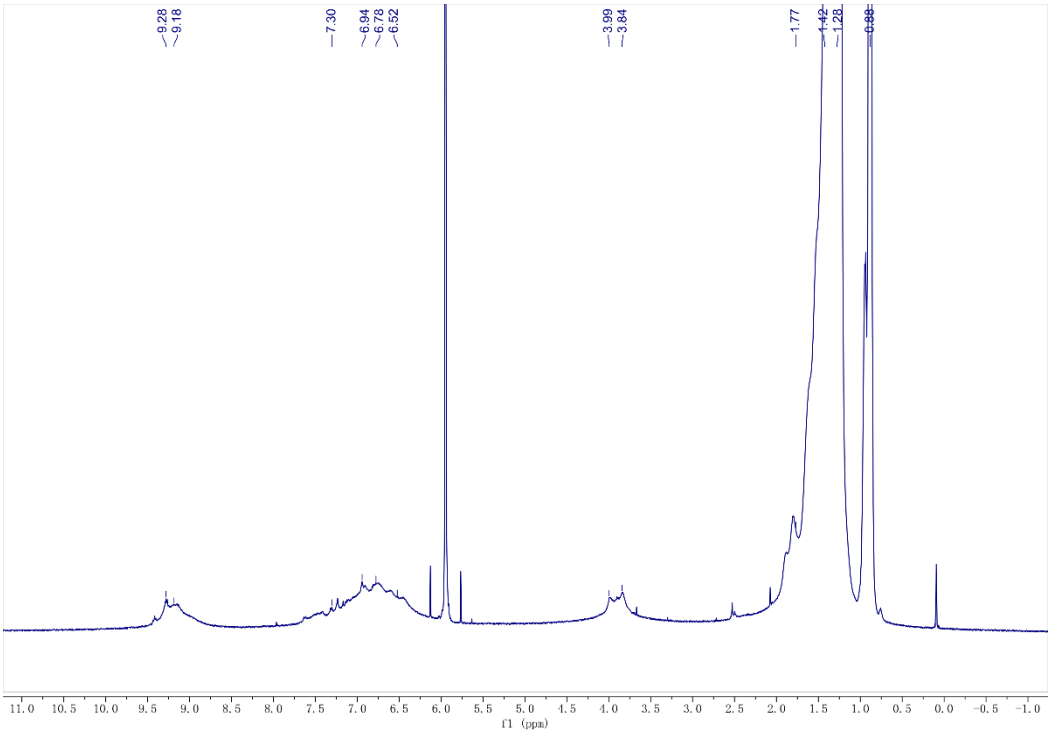

Figure S6. High temperature ^{1}H NMR spectrum of the bisisoindigo-based conjugated polymer **PNCCN-DTE**.

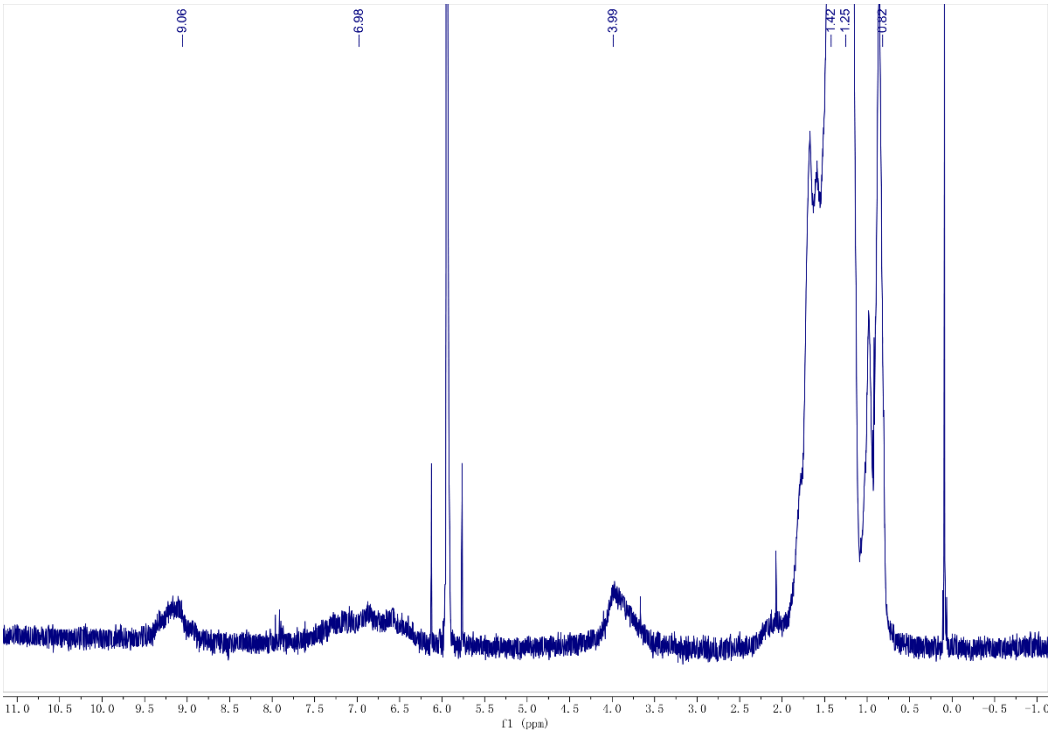

Figure S7. High temperature ^{1}H NMR spectrum of the bisisoindigo-based conjugated polymer **PNNNN-BT**.

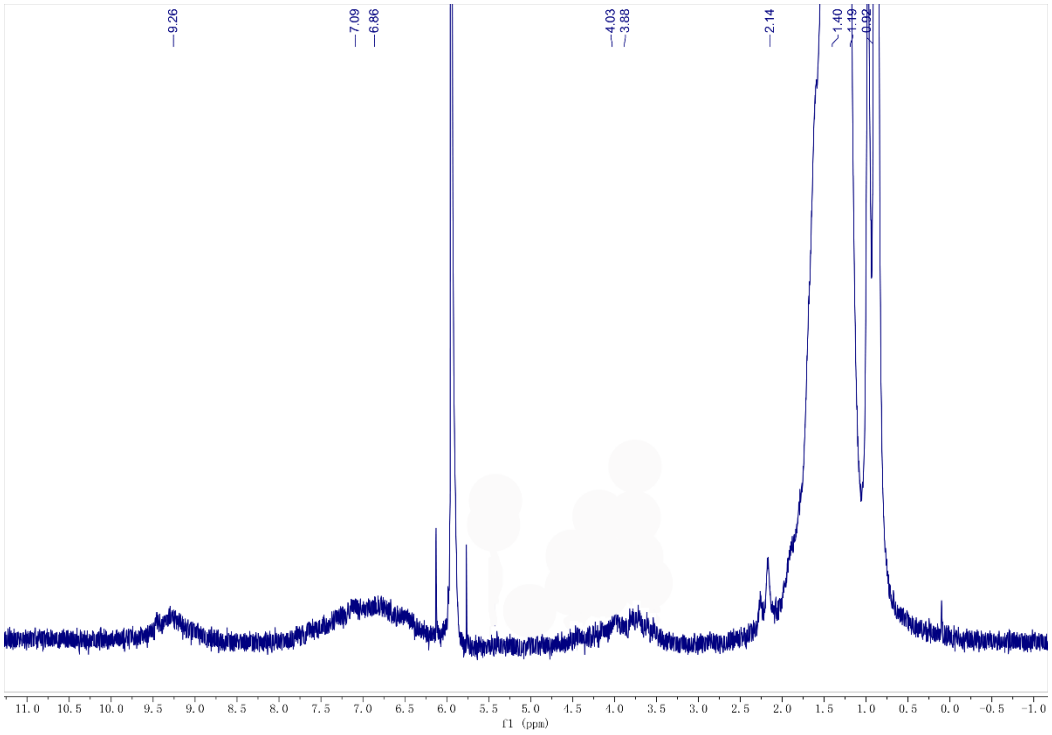

Figure S8. High temperature ^{1}H NMR spectrum of the bisisoindigo-based conjugated polymer **PNNNN-DTE**.

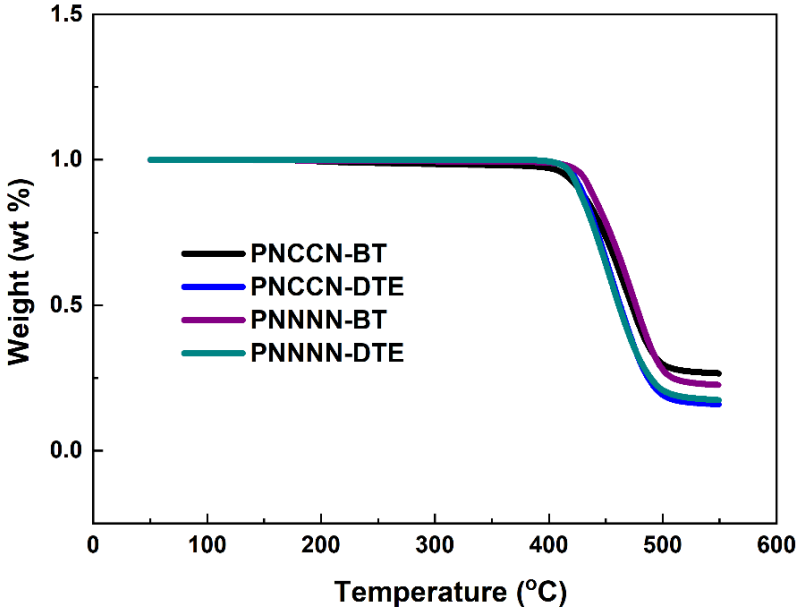

Figure S9. TGA traces of the bisisoindigo-based conjugated polymers **PNCCN-BT**, **PNCCN-DTE**, **PNNNN-BT**, and **PNNNN-DTE**.

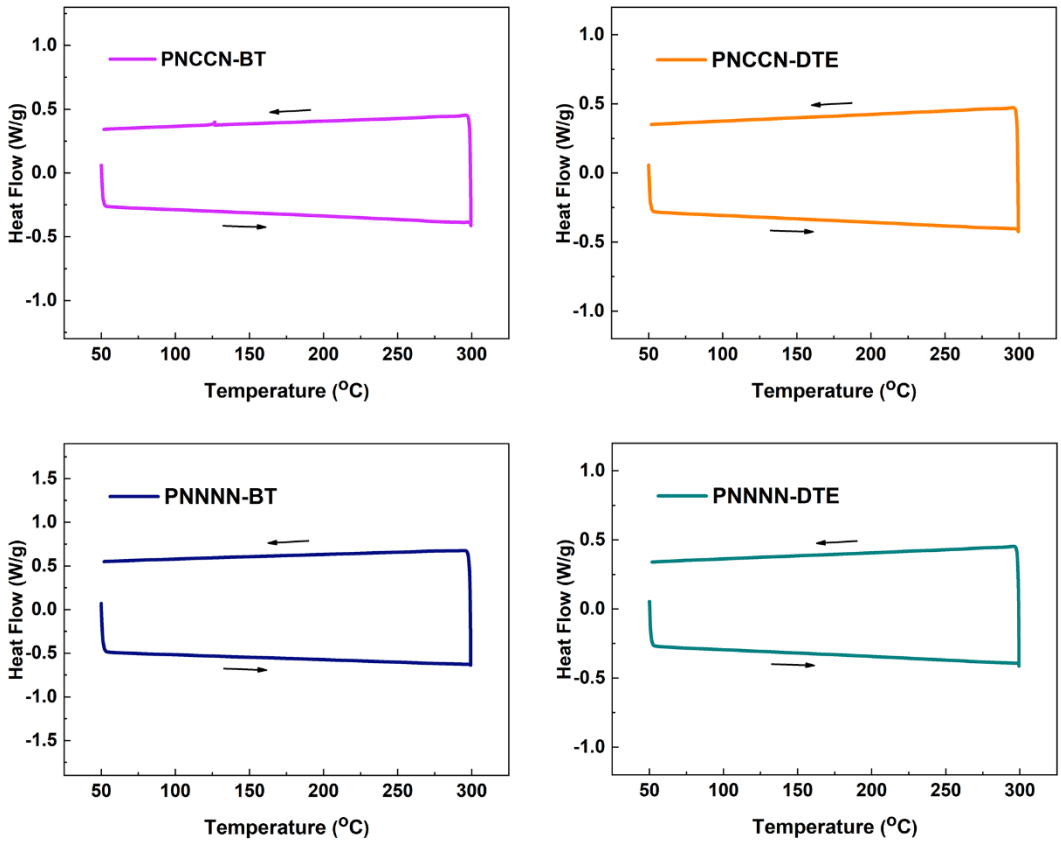

Figure S10. DSC curves of the bisisoindigo-based conjugated polymers **PNCCN-BT**, **PNCCN-DTE**, **PNNNN-BT**, and **PNNNN-DTE**.

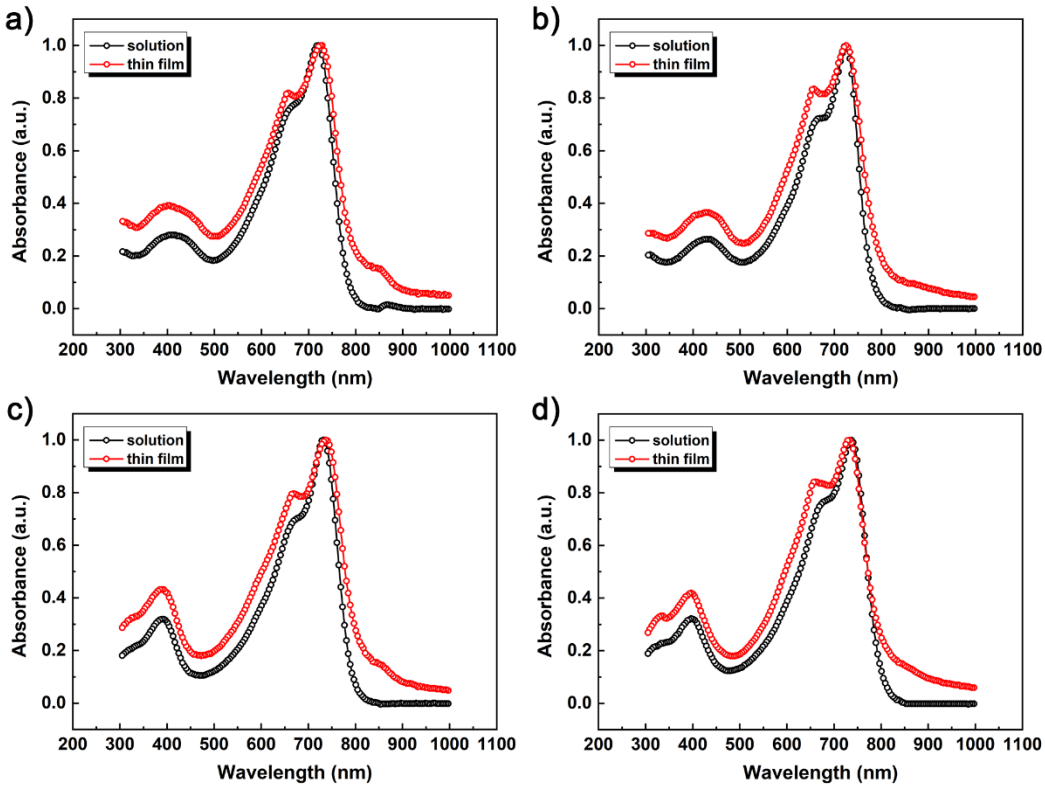

Figure S11. UV-vis-NIR absorption spectra of the bisisoindigo-based conjugated polymers a) **PNCCN-BT**, b) **PNCCN-DTE**, c) **PNNNN-BT**, and d) **PNNNN-DTE** in solution and as thin film spin-coated on quartz plates.

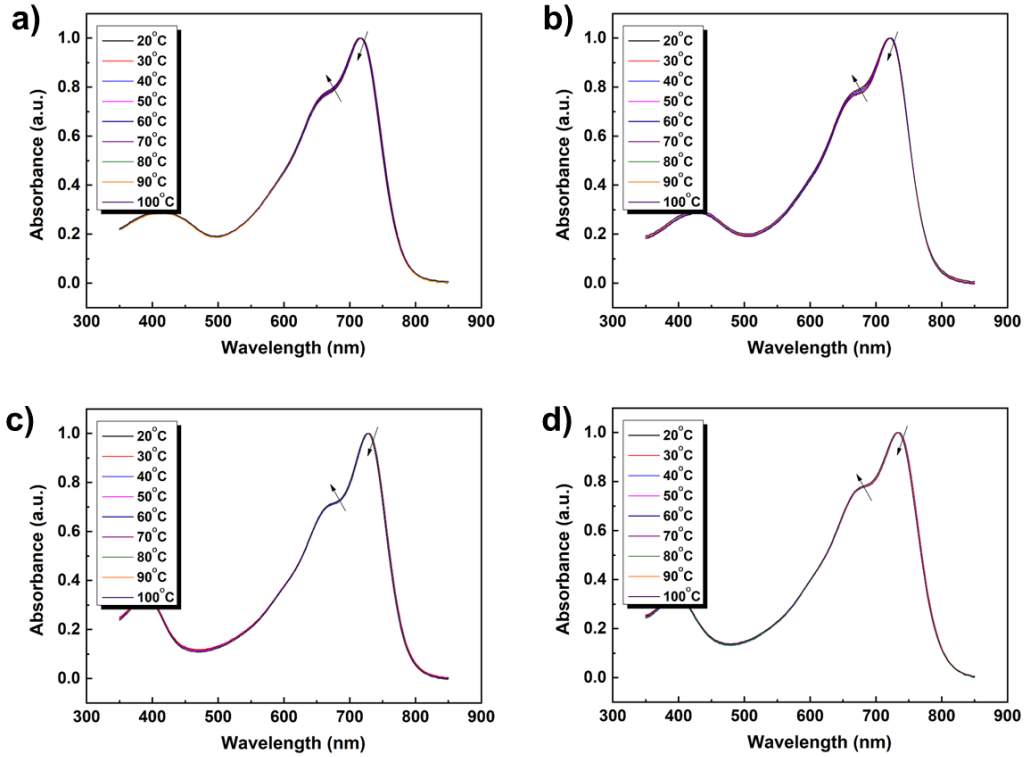

Figure S12. Temperature-dependent absorption spectra of the polymers in dilute chlorobenzene solution: a) **PNCCN-BT**, b) **PNCCN-DTE**, c) **PNNNN-BT**, d) **PNNNN-DTE**.

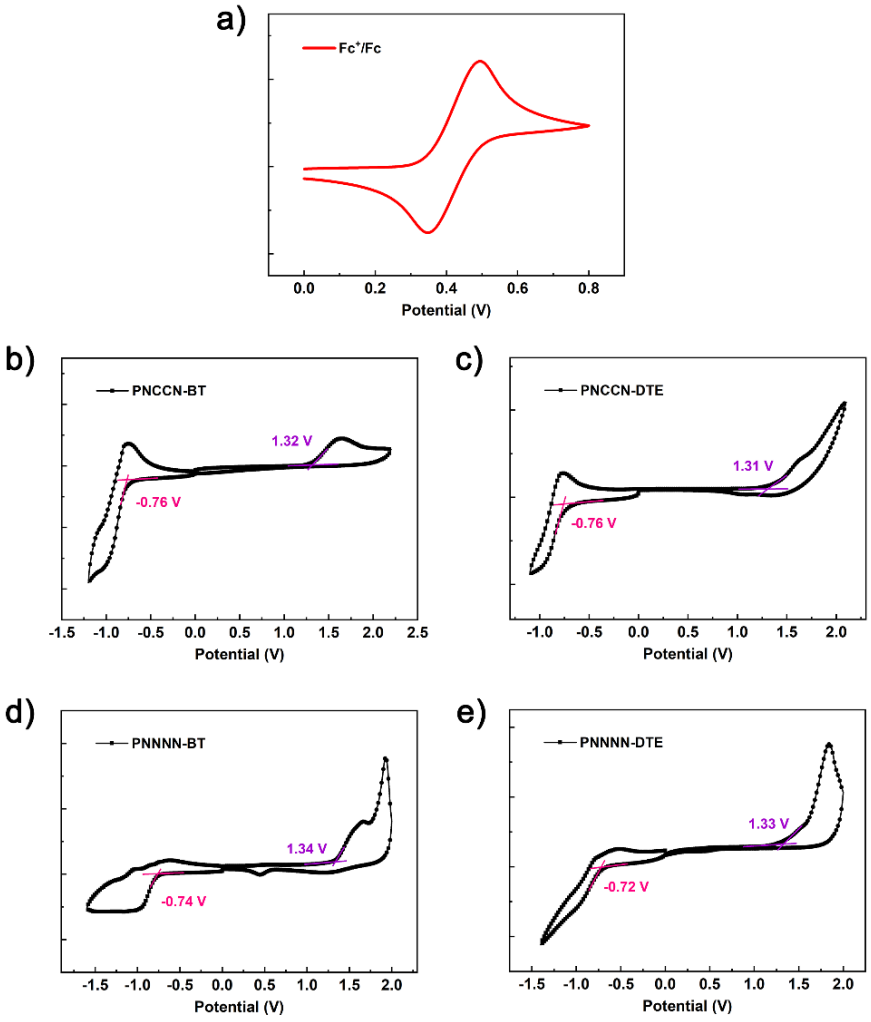

Figure S13. CV curves of a) ferrocene and the bisisoindigo-based conjugated polymers b) **PNCCN-BT**, c) **PNCCN-DTE**, d) **PNNNN-BT**, and e) **PNNNN-DTE**.

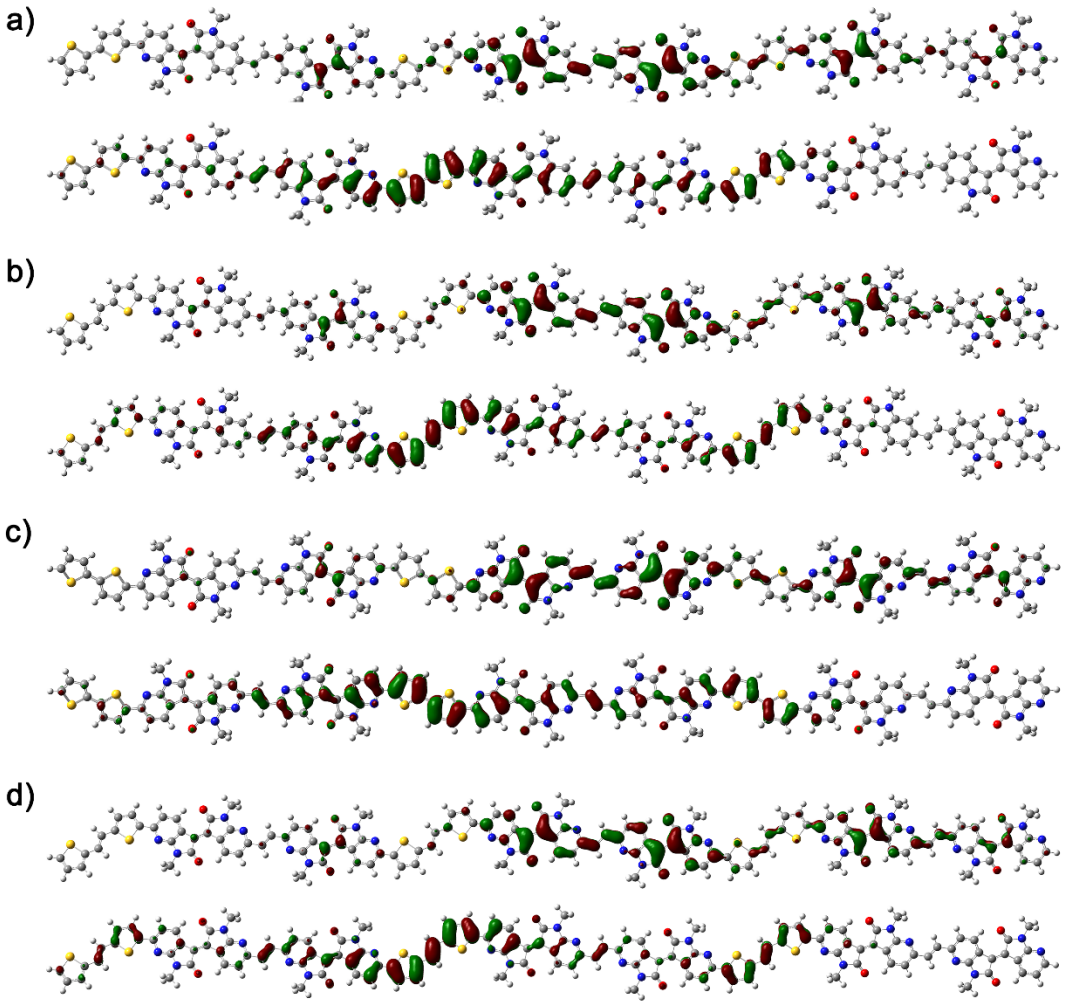

Figure S14. Computationally predicted molecular frontier orbitals of the bisisoindigo-based conjugated polymers a) **PNCCN-BT**, b) **PNCCN-DTE**, c) **PNNNN-BT**, and d) **PNNNN-DTE**. LUMO (up) and HOMO (down).

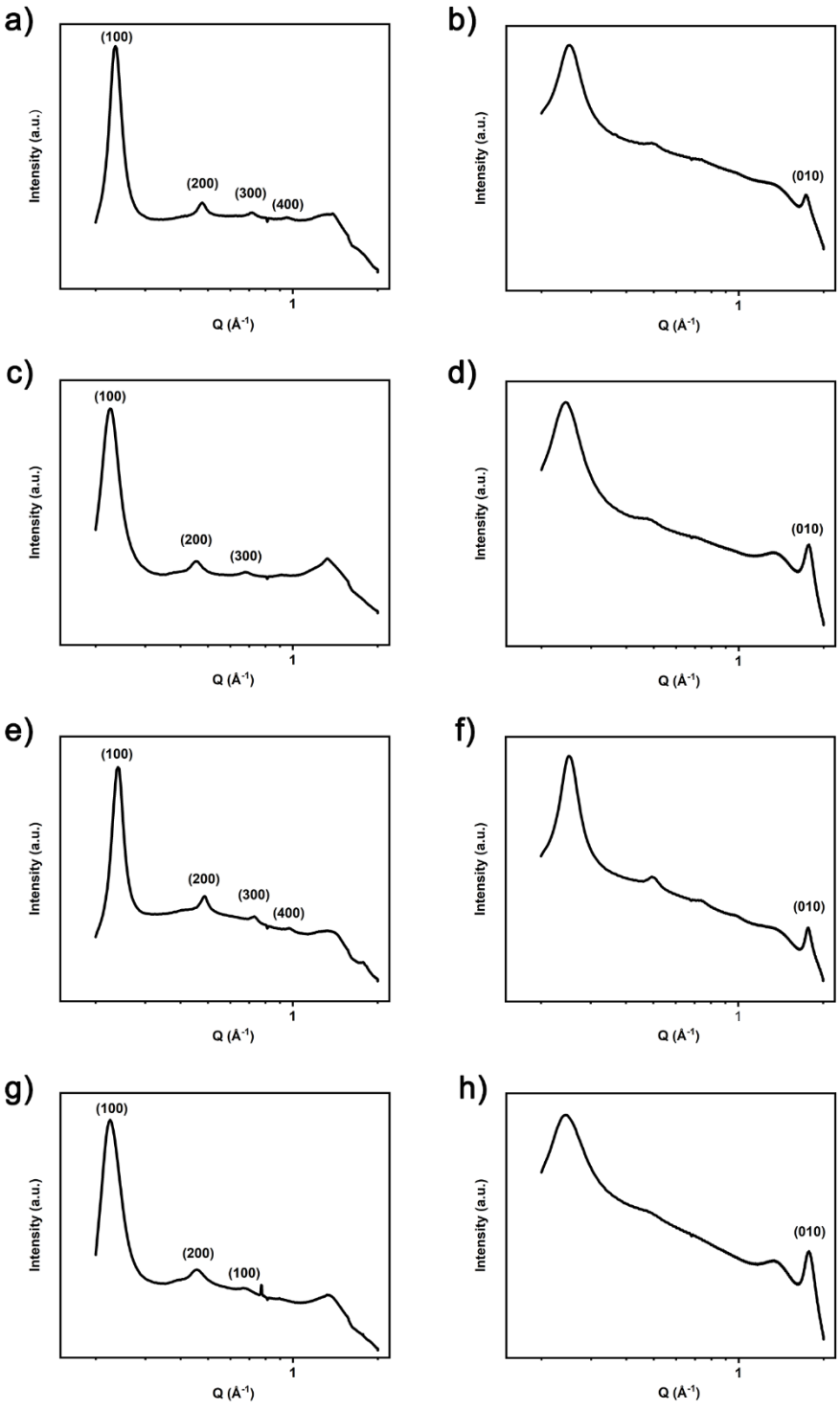

Figure S15. Out-of-plane and In-plane line profiles of the 2D-GIXRD patterns of the annealed a,b) **PNCCN-BT**, c,d) **PNCCN-DTE**, e,f) **PNNNN-BT**, g,h) **PNNNN-DTE** thin films prepared from DCB, a,c,e,g) out of plane and b,d,f,h) in-plane.

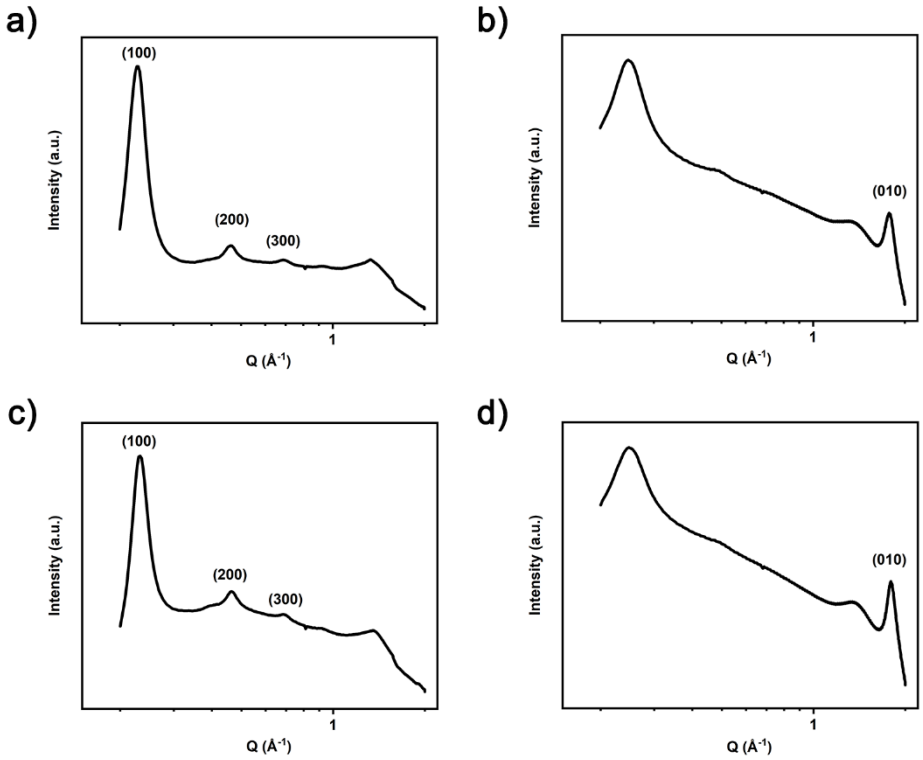

Figure S16. Out-of-plane and in-plane line profiles of the 2D-GIXRD patterns of the annealed a,b) **PNCCN-DTE**, and c,d) **PNNNN-DTE** thin films prepared from DCB/CN bi-component solvent (with v/v of 99.2/0.8), a,c) out of plane and b,d) in-plane.